

Simulation and control of a stand-alone pv- wind-battery-diesel generator hybrid power system

Hari Krishna Sabat¹, Pratap Chandra Pradhan²

M. Tech. student, student, Department of electrical engineering, DRIEMS, Cuttack, India¹

Associate Professor, Department of electrical engineering, DRIEMS, Cuttack, India²

ABSTRACT: As energy demands around the world increase, the need for renewable energy sources that will not harm the environment increases. Renewable energy, such as wind and solar energy, is desirable for power generation due to its unlimited existence and environmental friendly nature. This paper introduces a standalone hybrid power generation system consisting of solar and permanent magnet synchronous generator (PMSG) wind power sources and an AC load. Also there is two back up power supply sources i.e. Battery bank and Diesel Generator (DG) to supply the power during peak periods and when there is shortage of power occurs due to seasonal changes. Two contingencies are considered and categorized according to the power generation from each energy source, and the load requirement. In PV system Perturb & Observe (P&O) algorithm is used as control logic for the Maximum Power Point Tracking (MPPT) controller and Hill Climb Search (HCS) algorithm is used as MPPT control logic for the Wind power system in order to maximizing the power generated. The Fuzzy logic control scheme of the inverter is intended to keep the load voltage and frequency of the AC supply at constant level regardless of external climate conditions & load. A Simulink model of the proposed Hybrid system with the MPPT controlled Boost converters and Voltage regulated Inverter for stand-alone application is developed using MATLAB.

KEYWORDS: Hybrid energy, Solar PV, PMSG Wind, MPPT, inverter controller.

I. INTRODUCTION

During the past few years renewable energy sources have received greater attention and considerable efforts have been made to develop efficient energy conversion and utilization system. The major goals of these approaches are to have reduced environmental damage, conservation of energy, exhaustible sources and increased safety. The renewable energy systems can be used to supply power either directly to a utility grid or to an isolated load. The stand -alone system find wider applications as water pumps, for village electrification, supply of power to isolated areas which are far away from the utility grid. PV and Wind energy system are the most promising renewable energy technologies.

For renewable energy sources (RES) especially the variable speed wind energy conversion systems, Permanent Magnet Synchronous generator (PMSG) is gaining popularity. PMSG have a loss free rotor, and the power losses are confined to the stator winding and stator core. A multi-pole PMSG

connected to power converter can be used as direct driven PMSG in locations with low wind speed there by eliminating the gearbox which adds weight, losses, cost and maintenance. In a PV system, a solar cell alone can produce power of 1 to 2 watt. The solar cells are connected in series and parallel to form a PV panel or module or array. Thus a PV system consisting of PV array, Maximum Power Point Tracking (MPPT) boost converters, and Wind power system consisting of wind turbine, PMSG, rectifier and MPPT boost converter is integrated into Solar Wind hybrid power system (SWHPS). The output voltage of the PV and Wind power generation are quite low as compared with the desired operating level. So, this output voltage is brought to desired operating value of 220V using Boost converter with MPPT controller at each source.

The control logic of the MPPT controlled boost converter for the Wind power generation and PV based generation are selected on the basis of ease of implementation and robustness of the Hill Climb Search (HCS) and Perturb & Observe (P&O) algorithm respectively. The integration of renewable energy sources and energy storage systems has been one of the new trends in power electronic technology. Stand-alone wind with Solar Photovoltaic is known as the best hybrid combination of all renewable energy systems and suitable for most of the applications taking care of seasonal changes. They also complement each other during lean periods, for example additional energy production by wind during monsoon months compensates less output generated by solar. Similarly, in the post winter months when wind is dull, solar photovoltaic (SPV) takes over. This work proposes a solar PV and Wind generation based hybrid renewable energy system. The wind and solar systems are inter-connected with individual DC-DC converters and connected to the storage battery. The output of DC-DC converters is sent to an external inverter to supply ac power to load.

This paper deals with the simulation and control of PV-wind hybrid systems including energy storage battery and diesel generator (DG) connected to the AC load. Study of modelling and simulation on the entire PV/wind/battery/DG hybrid system is carried out under matlab /Simulink environment.

II. PHOTOVOLTAIC POWER SYSTEM

1. Single PV module modeling

The modeling of PV systems starts from the model of the elementary PV cell that is derived from that of the P-N

junction. The PV cell combines the behaviour of either voltage or current sources according to the operating point. This behaviour can be obtained by connecting a sunlight-sensitive current source with a P-N junction of a semiconductor material being sensitive to sunlight and temperature. The dotted line square in Fig. 1 shows the model of the ideal PV cell. The DC current generated by the PV cell is expressed as follows:

$$I = I_{PV} - I_S \left(e^{\frac{(V+I R_{se})}{aV_t}} - 1 \right) - \left(\frac{V+I R_{se}}{R_{sh}} \right) \dots\dots\dots 1$$

Where I_{pv} is the PV cell photocurrent, I_s is the diode current, V is the voltage across the diode, V_t is the PV cell thermal voltage, R_{se} is the series resistance, R_{sh} is the Shunt resistance, a is the ideality factor of the diode may be arbitrary chosen from the interval (1-1.5)

The light generated current of PV cell depends linearly on the irradiance and is also influenced by the temperature. It is given by:

$$I_{PV} = \left(\frac{G}{G_{STC}} \right) \{ I_{PVn} + K_i (T - T_{STC}) \} \dots\dots\dots 2$$

Where I_{PVn} is the nominal light-generated current provided at G_{STC} & T_{STC} , K_i is the cell's short circuit current temperature coefficient, G is the solar irradiance in W/m^2 , G_{STC} is the nominal solar irradiance in W/m^2 , T_{STC} is the temperature at standard test condition. The nominal light generated current is given by

$$I_{PVn} = \left(\frac{R_{se} + R_{sh}}{R_{se}} \right) I_{SCn} \dots\dots\dots 3$$

Where I_{SCn} is the nominal short circuit current or the maximum current available at the terminals of the practical device at nominal conditions.

The diode current I_s that is function of the voltage and current coefficients is given by the equation below:

$$I_s = \frac{I_{SCn} + K_T \Delta T}{e^{\frac{V_{OCn} + K_V \Delta T}{aV_t}} - 1} \dots\dots\dots 4$$

Where V_{OCn} is the voltage at short circuit standard test condition, K_V is the temperature coefficient of open circuit voltage.

2. Commercial PV module modeling

Commercially photovoltaic devices are available as sets of series and/or parallel-connected PV cells combined into one item, the PV module/array, to produce higher voltage and power, as shown in Fig.2. The equations of the PV array, considering shunt resistance infinity can be represented as

$$I = I_{PV} \cdot N_p - I_S \cdot N_p \left(e^{\frac{(V+I R_{se} N_s)}{aV_t N_s}} - 1 \right) \dots\dots\dots 5$$

Where V_T the PV cell thermal voltage given by $V_T = \frac{NsKT}{q}$, N_s is the number of cells connected in series for forming the PV module, N_p is the number of cells connected in parallel for forming the PV module, q is the charge of an electron.

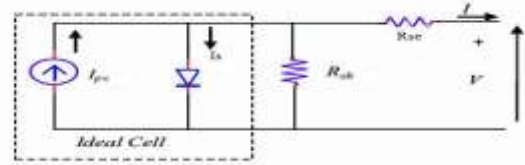


Fig. 1 Equivalent circuit of an ideal and practical PV cell

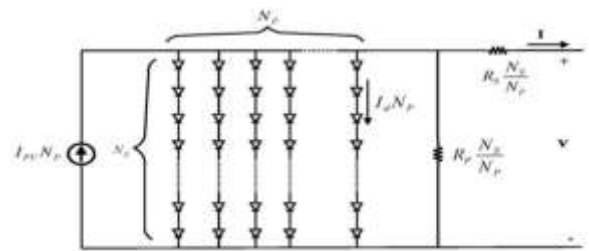


Fig. 2 Representation of PV module

3. I-V And P-V Characteristics

A PV module can be modeled as a current source that is dependent on the solar irradiance and temperature. The complex relationship between the temperature and irradiance results in a non-linear current-voltage characteristics. A typical I-V and P-V curve for the variations of irradiance and temperature is shown in Fig. 3 and 4, respectively. As can be observed, the MPP is not a fixed point; it fluctuates continuously as the temperature or the irradiance does. Due to this dynamics, the controller needs to track the MPP by updating the duty cycle of the converter at every control sample. A quicker response from the controller (to match the MPP) will result in better extraction of the PV energy and vice versa.

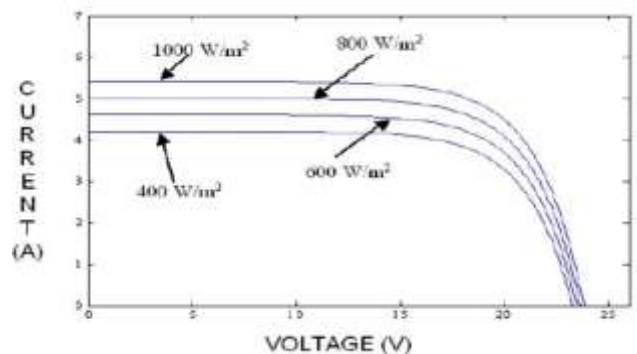


Fig. 3 Voltage-current characteristics of solar cell

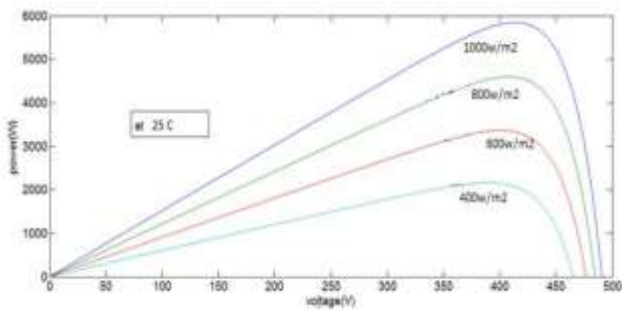


Fig. 4 voltage-power characteristics of PV cell

III. WIND POWER SYSTEM

Energy available in wind is basically the kinetic energy of large masses of air moving over the earth surface. Blades of the wind turbine receive this kinetic energy, which is then transformed to useful mechanical energy, which is then transformed further to mechanical or electrical energy depending on the end use. The actual power extracted by the rotor blades is the difference between the upstream and downstream wind powers is given by the following equation in units of watts:

$$P_o = 0.5 \times (\text{Mass flow per second}) \times (V^2 - V_o^2) \dots\dots\dots 6$$

Where P_o is the mechanical power extracted by the rotor, i.e., the turbine output power, V is the upstream wind velocity at the entrance of the rotor blades, and V_o is the downstream wind velocity at the exit of the rotor blades.

Macroscopically, the air velocity is discontinuous from V to V_o at the "plane" of the rotor blades, with an "average" of $\frac{1}{2}(V + V_o)$. The mechanical power extracted by the rotor, which drives the electrical generator, is therefore:

$$P_o = \frac{1}{2} \left[\rho A \frac{V+V_o}{2} \right] (V^2 - V_o^2) \dots\dots\dots 7$$

The preceding expression is algebraically rearranged in the following form:

$$P_o = \frac{1}{2} \rho A V^3 C_p = \frac{1}{2} \rho \cdot \pi R^2 \cdot V^3 C_p \dots\dots\dots 8$$

Where

$$C_p \left(\frac{\lambda}{\beta} \right) = \frac{\left(1 + \frac{V_o}{V}\right) \left[1 - \left(\frac{V_o}{V}\right)^2\right]}{2} \dots\dots\dots 9$$

Where ρ is the air density (kg/m³), A is the area swept by the rotor blades (m²), and β is the pitch angle (in degrees), R is the radius of the wind turbine blade, λ is the Tip Speed Ratio (TSR) and is given by $\lambda = \frac{\omega \cdot R}{V}$. The factor C_p is called the power coefficient of the rotor or the rotor efficiency.

The optimum value of C_p , say C_{pmax} , always occurs at a definite value of λ , say λ_{opt} which gives maximum power output as given by,

$$P_{max} = \frac{1}{2} \cdot \rho \cdot \pi \cdot R^5 \cdot \frac{C_{p,max}}{\lambda_{opt}^3} \times \omega^3 \dots\dots\dots 10$$

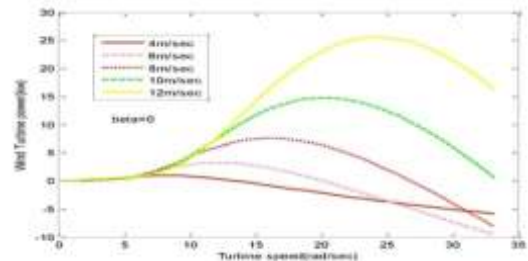


Fig.5 Characteristics of power vs. speed with different wind speed

IV. BACKUP POWER SUPPLY SYSTEM

1. Battery

The battery stores energy in an electrochemical form and is the most widely used device for energy storage in a variety of applications. The electric circuit-based models are useful to represent electrical characteristics of batteries. The simplest electric model consists of an ideal voltage source in series with an internal resistance. In this work, a generic battery model suitable for dynamic simulation presented in is considered. This model assumes that the battery is composed of a controlled-voltage source and a series resistance & typical discharge characteristics of NiCd battery, as shown below in Fig. 6 & 7 respectively.

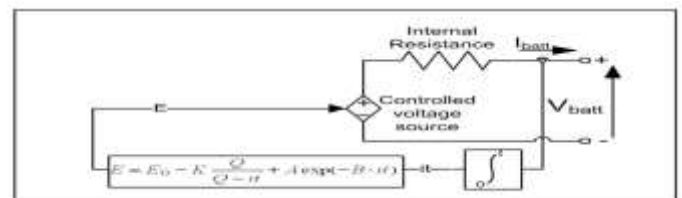


Fig. 6 A generic battery model.

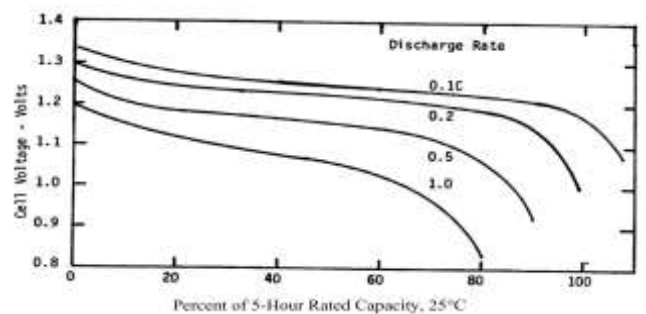


Fig. 7 Typical discharge characteristics of NiCd battery

2. Diesel Generator

A back up Diesel generator can be connected to the hybrid system to provide electric energy for peak loads which can't be covered by this hybrid system if a permanent electric power supply is required or in case of incapability of the renewable sources to supply the load. Diesel generator is used in the system to supply load when the output power from wind and PV is not enough to operate this load. The Diesel generator rating shall be large enough to achieve these tasks. Optimal unit sizing of a Diesel generator requires careful consideration of several factors including detailed analysis of daily and seasonal load fluctuations, annual load growth, and incorporation of practical constraints for feasible and reliable Diesel operation.

V. SYSTEM CONTROL

The configuration used to be evaluated in this thesis has a DC bus which combines the DC output of the PV module, the DC output of the wind turbine, and the battery bank. The AC bus of this configuration combines the output of the inverter, the output of the back-up diesel generator and the load. The AC loads are connected to the AC bus and DC loads are connected to the DC bus of the system. The block diagram of PV-wind hybrid power system is shown in below Fig. 8. The hybrid generations consist of Photovoltaic based generation, Wind Power Generation, Battery, Diesel Generator (DG), Voltage regulated inverter and AC load.

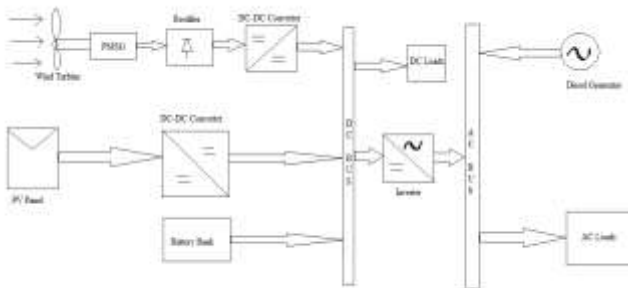


Fig. 8 Block diagram of PV-Wind-DG-Battery hybrid system

1. Perturb And Observe Mppt Algorithm For Pv Array

This method involves perturbation of the voltage, V, and observing the change in power output, P. If the perturbation in one direction increases the power output of the PV array, then the same direction of perturbation is continued. Otherwise, the direction of perturbation is reversed. Thus, it is a continuous process of searching for the voltage on power Vs voltage (P-V) curve, which increases the power output of the PV array. Fig. 9 below shows the p-v characteristics of a photovoltaic system, by analyzing the pv characteristics we can see that on right side of MPP as the voltage decreases the power increases but on left side of MPP increasing voltage will increase power. This is the main idea we have used in

the P&O algorithm to track the MPP . The flow chart of P&O algorithm is manifested in fig. 11.

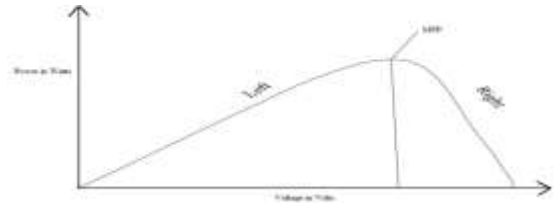


Fig. 9 P-V characteristics (basic idea of P&O algorithm)

2. Hill Climb Search (HCS) Method

HCS method of MPPT makes use of the inverted U shaped graph between power and rotor speed. As there is a definite peak power corresponding to a particular rotor speed, the

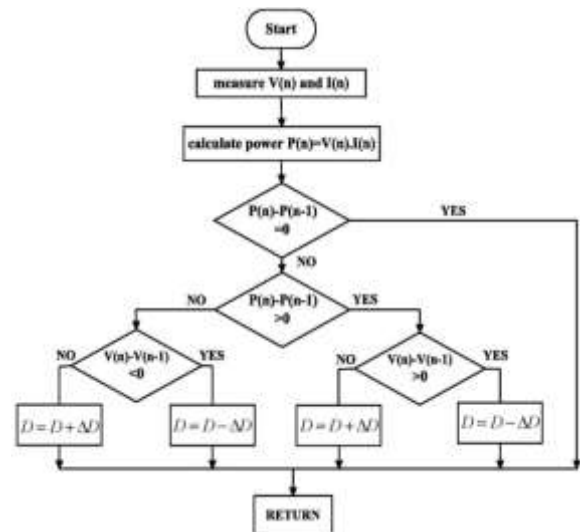


Fig. 11 The flow chart of P&O algorithm of solar pv system

algorithm compares the present power at an instant to the power obtained at the previous step. If the power is found to be increasing, then the duty cycle of the gating pulse applied to the converter switches are increased to drive the operating point more towards the peak power. If the power is found to be decreasing, then the duty cycle is reduced. In normal HCS methods the increments/decrements given to the duty cycle are fixed. The maximum power point is defined by the power curve in Fig.10 & the flowchart of proposed algorithm is as shown in Fig. 12.

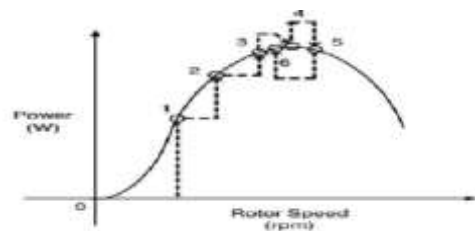


Fig. 10 Wind power curve for an arbitrary wind speed.

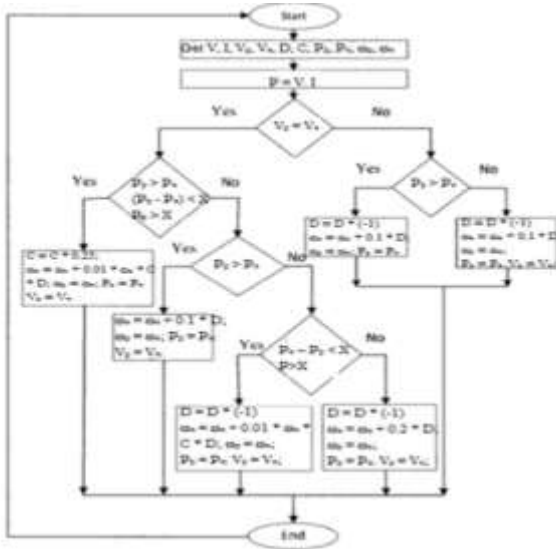


Fig. 12 Flowchart of proposed HCS MPPT algorithm

3. Voltage Regulated Inverter Design

The schematic diagram of Voltage regulated inverter is shown in Fig. 13.

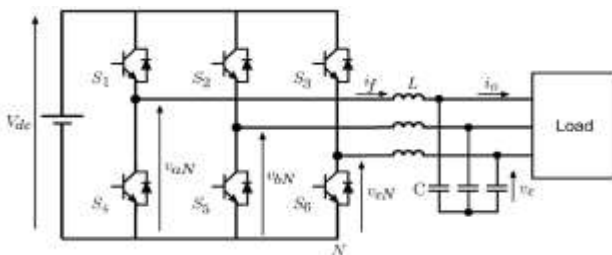


Fig. 13 Voltage Regulated inverter

The load voltage, frequency is controlled and maintained constant using inverter in stand-alone operation, so it plays an important role in the hybrid power generation. The rectified and boosted DC voltage from the PV, wind & battery is given as input to the inverter. Here, the proposed voltage regulated inverter maintains the output voltage and frequency constant irrespective of change in wind speed, solar irradiation levels and load conditions.

3.1 PI Voltage Regulated Inverter: The main work of voltage regulated inverter is to maintain the output voltage and frequency constant irrespective of change in wind speed, solar irradiation levels and load conditions. For achieving this, discrete Phase Lock Loop (PLL) with Synchronous Reference Frame (SRF) is implemented to generate control signal of the inverter. The output pulses of the PI controller is given as input gate signal of the inverter switches, which controls the output voltage and frequency of the inverter. Fig. 14 shows the block diagram of the PI control scheme of the inverter, where V_{Lab} , V_{Lbc} , V_{Lca} are the live voltages of the load.

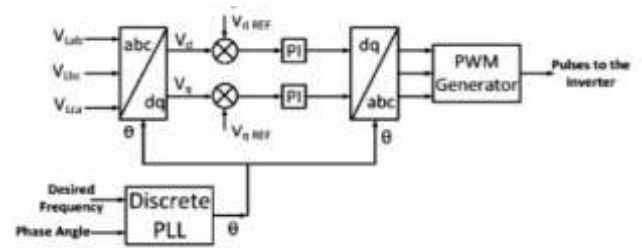


Fig. 14 Block diagram of PI voltage regulated inverter

3.2 Fuzzy Logic Voltage Regulated Inverter: Fuzzy logic control uses non-mathematical decision based algorithms that use operators' experiences. Fuzzy logic control is developed in this work to obtain desired output voltage of the chosen inverter. In the Fuzzy Implementation of mamdani FLC is selected and the inputs of the FLC are the error $e = V_{ref} - V_o$ and the change in error $ce = e_n - e_{n-1}$ where V_o is the actual output voltage of the inverter, V_{ref} is the desired output voltage and subscript n denotes sampling instances. δm_n is the change of modulation index inferred by the FLC at the n^{th} sampling instant. Using δm_n , the updated modulated signal m_s is obtained and fed to the SPWM generator which provides appropriate PWM signals m_n .

The crisp input values of 'e' and 'ce' are to be fuzzified and seven triangular membership functions are chosen in this work for simplicity. PB (Positive Big), PM (Positive Medium), PS (Positive Small), ZE (Zero), NS (Negative Small), NM (Negative Medium) and NB (Negative Big). The values of e, ce and δm_n are normalised to [-1, 1].

The block diagram of FLC voltage regulated inverter is shown in Fig. 15. Table 1 gives the rules for the mamdani FLC implemented. Fig. 16 shows the input membership functions for e and ce. The membership functions for change in modulation Index is shown in Fig. 17

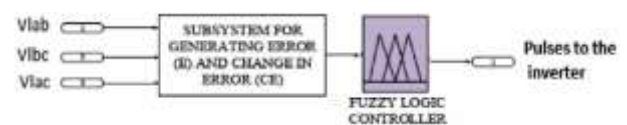


Fig. 15 Block diagram of FLC voltage regulated inverter.

Table 1 the rules for the mamdani FLC implemented.

e\ce	NB	NM	NS	ZE	PS	PM	PB
NB	NB	NB	NB	NB	NM	NS	ZE
NM	NB	NB	NB	NM	NS	ZE	PS
NS	NB	NB	NM	NS	ZE	PS	PM
ZE	NB	NM	NS	ZE	PS	PM	PB
PS	NM	NS	ZE	PS	PM	PB	PB
PM	NS	ZE	PS	PM	PB	PB	PB
PB	ZE	PS	PM	PB	PB	PB	PB

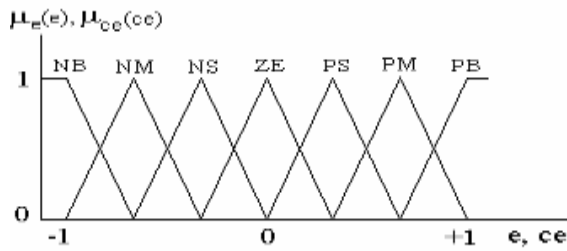


Fig. 16 Input membership functions for e and ce.

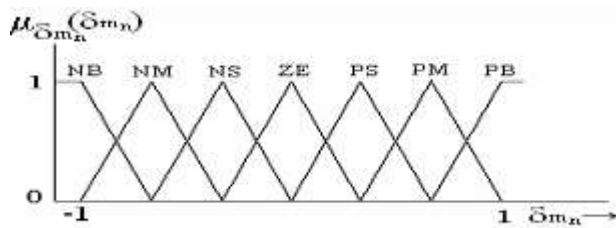


Fig. 17 Membership functions for change in modulation Index.

V. RESULT AND DISCUSSION

The solar PV power generation branch characteristics are analysed. Fig. 18 shows the change in irradiance level with time. Fig. 19 shows Output voltage for PV changing irradiation level. It clears that the PV power generation branch can perform the MPPT and achieves the maximum output power at a given irradiance level.

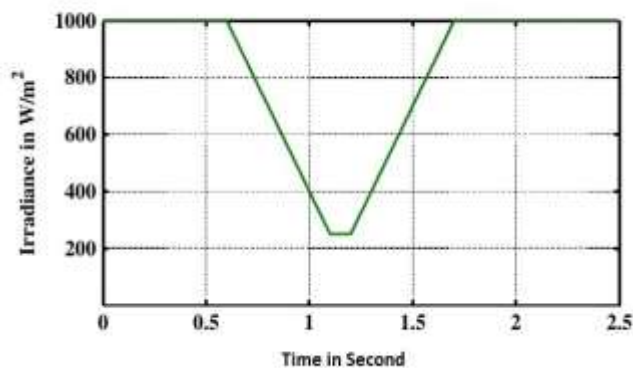


Fig. 28 PV changing irradiation level

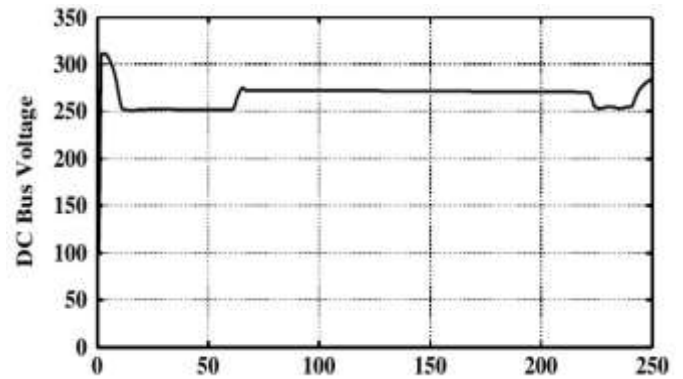


Fig. 19 Output voltage for PV changing irradiation level

The wind power generation branch characteristics are analysed. Fig. 20 shows the wind speed changing level with respect to time. Fig. 21 and 22 shows the output voltage & power for the PMSG wind system with HCS algorithm MPPT controller respectively.

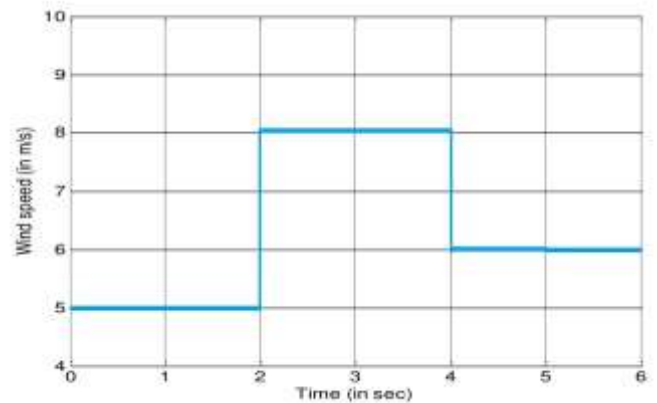


Fig. 20 Wind speed changing level

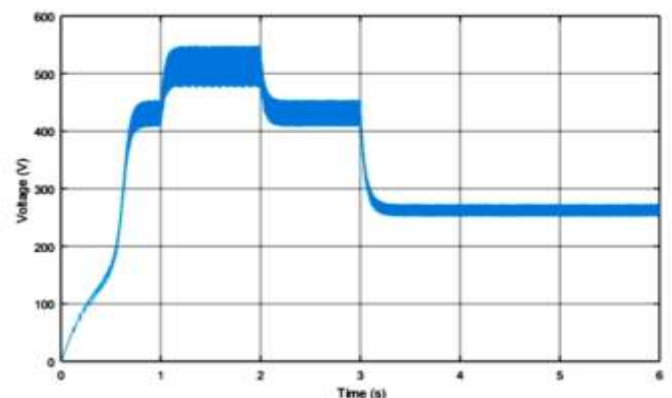


Fig. 21 Output Voltage wind

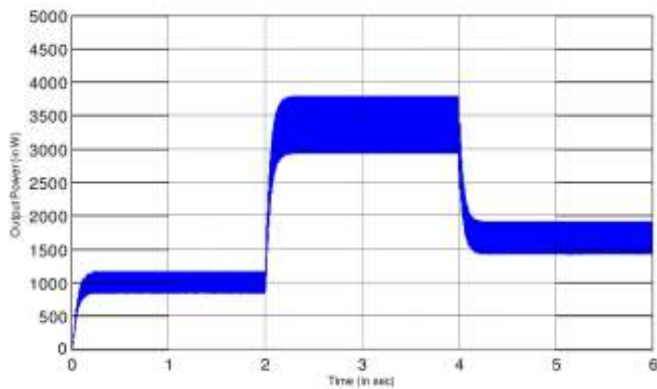


Fig. 22 Output power wind

From above it is clearly observed that the MPPT controller plays an important role in the hybrid power system. To reduce the losses and to improve the efficiency and performance of the hybrid system, we must have a faster MPPT controller.

The output voltage of the inverter is studied using PI controller and FLC. Figure 23 shows the Output voltage for inverter by using PI controller and figure 25 shows the output voltage for inverter by using FLC. In case-1, with PI voltage regulated inverter the output voltage is unstable with disturbance in frequency compared to the FLC voltage regulated inverter. The power generation of the hybrid system under varying wind speed and irradiation in case of PI control and FLC is shown in figure 24 and figure 26 respectively.

Case 1: PI Voltage Regulated Inverter

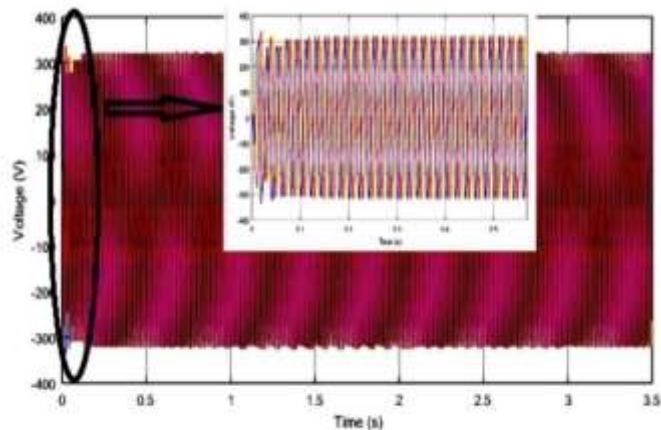


Fig. 23 Output voltage for inverter

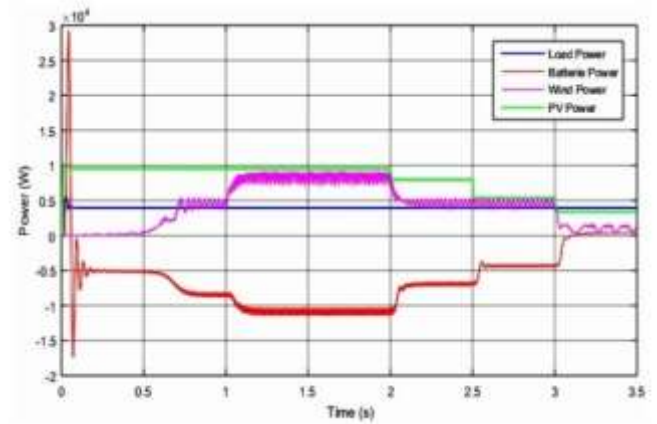


Fig. 24 Power generation of the hybrid system under varying wind speed and irradiation

Case 2: Fuzzy Logic Voltage Regulated Inverter

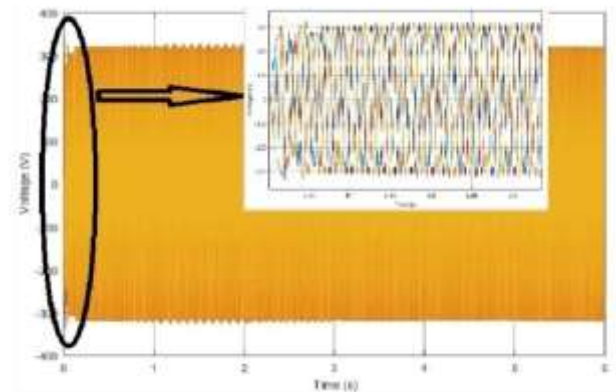


Fig. 25 Output voltage for inverter

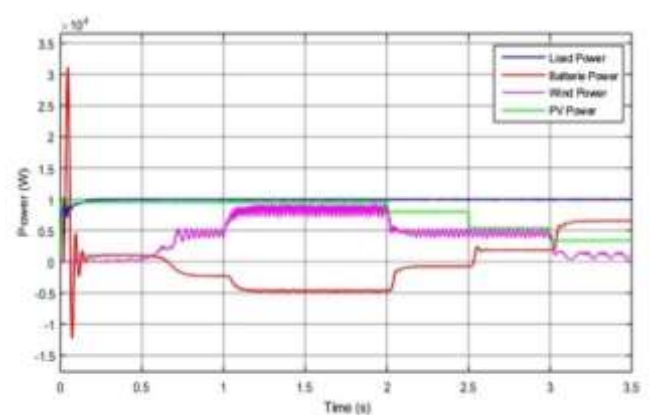


Fig. 26 Power generation of the hybrid system under varying wind speed and irradiation

The power flow in the second case provide the power efficiency and the advantage of fuzzy logic controller algorithm to control the inverter and the stability of system compared to the PI voltage regulated inverter.

VI. CONCLUSION

A hybrid power generation system which comprises of PV arrays, wind turbines and diesel generator with battery banks and power conditioning units has been discussed in this thesis.

- PV cell, module and array are simulated and effect of environmental conditions on their characteristics is studied.
- Wind energy system has been studied and simulated.
- Maximum power point of operation is tracked for both the systems using P&O algorithm.
- Both the systems are integrated and the hybrid system is used for battery charging and discharging.
- The diesel generator is used for supplying power to the load during peak load period & bad climate conditions when there is lack of power of pv-wind-battery hybrid system. Also the diesel generator supplies power to the load during maintenance work of the system.
- The PI and fuzzy controllers developed have been tested through simulation for regulating output voltage and minimizing the harmonics of the chosen inverter.
- FLC voltage regulated inverter is more power efficiency and reliable compared to the PI voltage regulated inverter, in this context FLC improve the effect of the MPPT algorithm in the power generation system of which sources solar and wind power generation systems.

REFERENCES

- [1] Seul Ki Kim, Eung Sang Kim, Jong Bo Ahn, "Modelling and control of a Grid connected Wind/PV Hybrid Generation System", 2005/2006 IEEE PES Transmission and Distribution Conference and Exhibition, 21-24 May 2006, pp.1202-1207.
- [2] N. Pandiarajan, Ranganath Muthu, "Mathematical Modelling of Photovoltaic Module with Simulink", First International Conference on Electrical energy system (ICEES), 3-5 January 2011, pp.258-263.
- [3] Munish Kumar, "Simulation and Analysis of Grid Connected Photovoltaic System with MPPT", 2012 IEEE 5th Power India Conference, 19-22 dec.2012, pp.1-6.
- [4] Kun Ding, Xin Gao Bian, "A MATLAB-Simulink-Based PV Module Model and its Application Under Conditions of Non uniform Irradiance", IEEE Transactions On Energy Conversion, Vol.27, NO.4, December 2012.
- [5] Ling Lu, Ping Liu, "Research and Simulation on Photovoltaic Power System Maximum Power Control" international conference on Electrical and control Engg. (ICECE), 16-18 sept.2011, pp. 1394-1398.
- [6] Dezso Sera, Laszlo Mathe, Tamas Kerekes, "On the Perturb-and-Observe and Incremental Conductance MPPT Methods for PV Systems", July 2013 IEEE Journal of Photovoltaic, VOL.3, no.3, pp.1070-1078.
- [7] Natsheh, E.M.; Albarbar, A.; Yazdani, J., "Modelling and control for smart grid integration of solar/wind energy conversion system," 2nd IEEE PES International Conference and Exhibition on Innovative Smart Grid Technologies (ISGT Europe), pp.1-8, 5-7 Dec. 2011.
- [8] Sibasish Panda, Anup Kumar Panda, "Fault Analysis on Grid Connected MPPT based Photovoltaic System", 2013 International journal of Current Engineering and Technology.
- [9] Kurozumi, Kazuhiro et al, "Hybrid system composed of a wind power and a photovoltaic system at NTT Kumejima radio relay station", INTELEC, International Telecommunications Energy Conference 1998, pp. 785-789.
- [10] J.G. Sloopweg, H. Polinder, W.L. Kling "Representing Wind Turbine electrical generating system in fundamental frequency simulation", IEEE Trans. on energy conversion, Vol.18, No.4, December 2003, pp.516-524.
- [11] S. M. Shaahid and M. A. Elhadidy, "Opportunities for utilization of stand-alone hybrid (photovoltaic + diesel + battery) power systems in hot climates," Renewable Energy, vol. 28, no. 11, pp. 1741-1753, 2003.
- [12] T. Esram, P.L. Chapman, "Comparison of Photovoltaic Array Maximum Power Point Tracking Techniques," IEEE Transactions on Energy Conversion, vol. 22, no. 2, pp. 439-449, June 2007.